titis C. Gut 2007; 56: 553—559
41) Mangia A, Minerva N, Bacca D, et al. Determinants of relapse after a short (12 weeks) course of antiviral therapy and re-treatment efficacy of a prolonged course in patients with chronic hepatitis C virus genotype 2 or 3 infection. Hepatology 2009; 49: 358—363
42) Akuta N, Suzuki F, Kawamura Y, et al. Predictors of viral kinetics to peginterferon plus ribavirin combination therapy in Japanese patients infected with hepatitis C virus genotype 1b. J Med Virol 2007; 79: 1686—1695
43) Helbling B, Jochum W, Stamenic I, et al. HCV-related advanced fibrosis/cirrhosis: randomized controlled trial of pegylated interferon alpha-2a and ribavirin. J Viral Hepat 2006; 13: 762—769
44) Bergmann JF, Vrolijk JM, van der, Schaar P, et al. Gamma-glutamyltransferase and rapid virological response as predictors of successful treatment with experimental or standard peginterferon-alpha-2b in chronic hepatitis C non-responders. Liver Int 2007; 27: 1217—1225
45) Diago M, Crespo J, Olveira A, et al. Clinical trial: pharmacodynamics and pharmacokinetics of re-treatment with fixed-dose induction of peginterferon alpha-2a in hepatitis C virus genotype 1 true non-responder patients. Aliment Pharmacol Ther 2007; 26: 1131—1138
46) Carr C, Hollinger FB, Yoffe B, et al. Efficacy of interferon alpha-2b induction therapy before retreatment for chronic hepatitis C. Liver Int 2007; 27: 1111—1118
47) Mathew A, Peiffer LP, Rhoades K, et al. Sustained viral response to pegylated interferon alpha-2b and ribavirin in chronic hepatitis C refractory to prior treatment. Dig Dis Sci 2006; 51: 1956—1961
48) Jacobson IM, Gonzalez SA, Ahmed F, et al. A randomized trial of pegylated interferon alpha-2b plus ribavirin in the retreatment of chronic hepatitis C. Am J Gastroenterol 2005; 100: 2453—2462
49) Herrine SK, Brown RS Jr, Bernstein DE, et al. Peginterferon alpha-2a combination therapies in chronic hepatitis C patients who relapsed after or had a viral breakthrough on therapy with standard interferon alpha-2b plus ribavirin: a pilot study of efficacy and safety. Dig Dis Sci 2005; 50: 719—726
50) Shiffman ML, Di Bisceglie AM, Lindsay KL, et al. Peginterferon alfa-2a and ribavirin in patients with chronic hepatitis C who have failed prior treatment. Gastroenterology 2004; 126: 1015—1023
51) Jensen DM, Marcellin P, Freilich B, et al. Re-treatment of patients with chronic hepatitis C who do not respond to peginterferon-alpha2b: a randomized trial. Ann Intern Med 2009; 150: 528—540
52) Poynard T, Colombo M, Bruix J, et al. Peginterferon alfa-2b and ribavirin: effective in patients with hepatitis C who failed interferon alfa/ribavirin therapy. Gastroenterology 2009; 136: 1618—1628
53) 熊田博光.「厚生労働科学研究費補助金　肝炎等克服緊急対策事業（肝炎分野）肝硬変を含めたウイルス性肝疾患の治療の標準化に関する研究　平成20年度総括・分担報告書」
54) Kamal SM. Acute hepatitis C: a systematic review. Am J Gastroenterol 2008; 103: 1283—1297
55) Nishiguchi S, Kuroki T, Nakatani S, et al. Randamised trial of effects of interferon-α on incidence of hepatocellular carcinoma in chronic active hepatitis C with cirrhosis. Lancet 1995; 346: 1051—1055
56) Arase Y, Ikeda K, Suzuki F, et al. Prolonged-interferon therapy reduces hepatocarcinogenesis in aged-patients with chronic hepatitis C. J Med Virol 2007; 79: 1095—1102
57) Kubo S, Nishiguchi S, Hirohashi K, et al. Effects of long-term postoperative interferon-alpha therapy on intrahepatic recurrence after resection of hepatitis C virus-related hepatocellular carcinoma. A randomized, controlled trial. Ann Intern Med 2001; 134: 963—967
58) Shiratori Y, Shiina S, Teratani T, et al. Interferon therapy after tumor ablation improves prognosis in patients with hepatocellular carcinoma associated with hepatitis C virus. Ann Intern Med 2003; 138: 299—306
59) Di Bisceglie AM, Shiffman ML, Everson GT, et al. Prolonged therapy of advanced chronic hepatitis C with low-dose peginterferon. N Engl J Med 2008; 359: 2429—2441
60) Yamada G, Iino S, Okuno T, et al. Virological response in patients with hepatitis C virus genotype 1b and a high viral load: impact of peginterferon-

alpha-2a plus ribavirin dose reductions and host-related factors. Clin Drug Investig 2008; 28: 9—16
61) Oze T, Hiramatsu N, Yakushijin T, et al. Pegylated interferon alpha-2b affects early virologic response dose-dependently in patients with chronic hepatitis C genotype 1 during treatment with Peg-IFN alpha-2b plus ribavirin. J Viral Hepat 2009; 16: 578—585
62) Hiramatsu N, Oze T, Yakushijin T, et al. Ribavirin dose reduction raises relapse rate dose-dependently in genotype 1 patients with hepatitis C responding to pegylated interferon alpha-2b plus ribavirin. J Viral Hepat 2009; 16: 586—594
63) Mangia A, Santoro R, Minerva N, et al. Peginterferon alfa-2b and ribavirin for 12 vs. 24 weeks in HCV genotype 2 or 3. N Engl J Med 2005; 352: 2609—2617
64) Weiland O, Hollander A, Mattsson L, et al. Lower-than-standard dose peg-IFN alfa-2a for chronic hepatitis C caused by genotype 2 and 3 is syfficient when given in combination with weight-based ribavirin. J Viral Hepati 2008; 15: 641—645
65) Inoue Y, Hiramatsu N, Oze T, et al. Factors affecting efficacy in patients with genotype 2 chronic hepatitis C treated by pegylated interferon alpha-2b and ribavirin: reducing drug doses has no impact on rapid and sustained virological responses. J Viral Hepat in press.
66) McHutchison JG, Everson GT, Gordon SC, et al. Telaprevir with peginterferon and ribavirin for chronic HCV genotype 1 infection. N Engl J Med 2009; 360: 1827—1838

JSH Consensus Kobe 2009: Diagnosis and Treatment of Hepatitis C

Shuhei Nishiguchi[1]*, Namiki Izumi[2], Keisuke Hino[3], Fumitaka Suzuki[4], Hiromitsu Kumada[4], Yoshito Ito[5], Yasuhiro Asahina[2], Akihiro Tamori[6], Naoki Hiramatsu[7], Norio Hayashi[7], Masatoshi Kudo[8]

Key words: chronic hepatitis C diagnosis guideline treatment

Kanzo 2009; 50: 665—677

1) Hyogo Medical University
2) Musashino Red Cross Hospital
3) Kawasaki Medical University
4) Toranomon Hospital
5) Kyoto Prefectural University of Medicine
6) Osaka City University
7) Osaka University
8) Kinki University
*Corresponding author: nishiguc@hyo-med.ac.jp

Liver International ISSN 1478-3223

BASIC STUDIES

Hepatitis C virus protein and iron overload induce hepatic steatosis through the unfolded protein response in mice

Sohji Nishina[1,2], Masaaki Korenaga[1,2], Isao Hidaka[1], Akane Shinozaki[3], Aya Sakai[3], Toshikazu Gondo[4], Mitsuaki Tabuchi[5], Fumio Kishi[5] and Keisuke Hino[2,3]

1 Department of Gastroenterology and Hepatology, Yamaguchi University Graduate School of Medicine, Kawasaki Medical University, Okayama, Japan
2 Department of Internal Medicine, Division of Hepatology and Pancreatology, Kawasaki Medical University, Okayama, Japan
3 Department of Basic Laboratory Sciences, Yamaguchi University Graduate School of Medicine, Kawasaki Medical University, Okayama, Japan
4 Department of Surgical Pathology, Yamaguchi University Hospital, Yamaguchi, Kawasaki Medical University, Okayama, Japan
5 Department of Molecular Genetics, Kawasaki Medical University, Okayama, Japan

Keywords
endoplasmic reticulum stress – hepatic steatosis – hepatitis C virus – iron – unfolded protein response

Abbreviations
ATF6, activating transcription factor 6; CHOP, CCAAT/enhancer-binding protein homology protein; CPTI, carnitine palmitoyl transferase I; ER, endoplasmic reticulum; FAS, fatty acid synthetase; HCC, hepatocellular carcinoma; HCV, hepatitis C virus; IRE1, inositol-requiring enzyme1; NAC, *N*-acetyl cysteine; p-eIF2α, phosphorylated eukaryotic initiation factor-2α; PERK, PKR-like ER kinase; PKR, RNA-activated protein kinase; ROS, reactive oxygen species; SCAP, SREBP cleavage-acting protein; SREBP, sterol-regulatory element-binding protein; XBP-1, X-box DNA-binding protein 1.

Correspondence
Keisuke Hino, Department of Internal Medicine, Division of Hepatology and Pancreatology, Kawasaki Medical University, 577 Matsushima, Kurashiki, Okayama, 701-0192, Japan
Tel: +81 86 4621111
Fax: +81 86 4641196
e-mail: khino@med.kawasaki-m.ac.jp

Received 29 July 2009
Accepted 12 January 2010

DOI:10.1111/j.1478-3231.2010.02210.x

Abstract

Background/Aim: Hepatic iron overload and steatosis play critical roles in the progression of hepatitis C virus (HCV)-associated chronic liver disease. However, how these two pathophysiological features affect each other remains unknown. The aim of this study was to investigate how hepatic iron overload contributes to the development of hepatic steatosis in the presence of HCV proteins. *Methods:* Male C57BL/6 transgenic mice expressing the HCV polyprotein and nontransgenic littermates were fed an excess-iron diet or a control diet. Mice in each group were assessed for the molecules responsible for fat accumulation in the liver. *Results:* Hepatic iron levels were positively correlated with triglyceride concentrations in the liver for all mice. As compared with the livers of nontransgenic mice fed the control diet, the livers of transgenic mice fed the iron-excess diet showed a lower expression of carnitine palmitoyl transferase I, a higher expression of sterol-regulatory element-binding protein 1 and fatty acid synthetase and an activated unfolded protein response, indicated by a higher expression of unspliced and spliced X-box DNA-binding protein 1 (XBP-1), phosphorylated eukaryotic initiation factor-2α (p-eIF2α), CCAAT/enhancer-binding protein homology protein (CHOP) and abundant autophagosomes concomitant with increased production of reactive oxygen species. Six-month treatment with the anti-oxidant N-acetyl cysteine dramatically reduced hepatic steatosis in transgenic mice fed the iron-excess diet through decreased expression of unspliced and spliced XBP-1, p-eIF2α, and CHOP. *Results:* The iron-induced unfolded protein response appears to be one of the mechanisms responsible for fat accumulation in the liver in transgenic mice expressing the HCV polyprotein.

Hepatic steatosis and iron overload are not only the pathophysiological features of hepatitis C virus (HCV)-associated chronic liver disease (1, 2) but also risk factors for the development of hepatocellular carcinoma (HCC) (3, 4). Thus, these pathophysiological features appear to play critical roles in the pathogenesis of HCV-associated chronic liver disease. The mechanisms underlying HCV-related steatosis are diverse. HCV core protein has been demonstrated to inhibit microsomal transfer protein activity and very low-density lipoprotein secretion (5) and to upregulate the promoter activity of sterol-regulatory element-binding protein (SREBP) 1c, a transcription factor involved in lipid synthesis (6). Persistent activation of peroxisome proliferator-activated receptor α has also been reported to be essential for the development of hepatic steatosis in transgenic mice expressing the HCV core protein (7). As for hepatic iron overload, we have shown that HCV-induced reactive oxygen species (ROS) increase the hepatic iron concentration by reducing hepcidin transcription in transgenic mice expressing the HCV polyprotein (8), and that even modest iron supplementation results in the development of liver tumours,

including HCC, through mitochondrial injury in these transgenic mice (9). However, it remains unknown how these two pathophysiological features affect each other in the progression of HCV-associated chronic liver disease. In our previous study, marked hepatic steatosis was observed at 6 months after commencement of iron overloading in transgenic mice, which was followed by the development of liver tumours. These results clearly indicated that hepatic iron overload was involved in the development of hepatic steatosis in the presence of HCV proteins. The aim of this study was to investigate how hepatic iron overload contributes to the development of hepatic steatosis in transgenic mice expressing the HCV polyprotein. In the present study, we report that iron-induced ROS-activated unfolded protein response may be postulated as one of the possible mechanisms of HCV-related fat accumulation in the liver.

Materials and methods

Animals

The transgene pAlbSVPA-HCV, containing the full-length polyprotein-coding region under the control of the murine albumin promoter/enhancer, was described in detail (10, 11). HCV polyprotein has been demonstrated to be processed into individual proteins in the liver and to be expressed at a biologically relevant level in which transcripts of RNA encoding the complete viral polyprotein are detectable only by a reverse-transcription polymerase chain reaction (11). Of the four transgenic lineages with evidence of RNA transcription of the full-length HCV-N open reading frame (FL-N), the FL-N/35 lineage proved capable of breeding in large numbers. There is no inflammation in the transgenic liver (11). Male FL-N/35 transgenic mice and age-matched C57BL/6 mice (control mice) were fed a normal rodent diet including carbonyl iron (45 mg/kg diet, control diet) or an iron-excess diet (carbonyl iron 225 mg/kg diet) at the age of 8 weeks, bred, maintained and killed by an intraperitoneal injection of 10% pentbarbital sodium preceded by 12-h fasting at 12 months after initiation of feeding according to the criteria outlined in the Guide for the Care and Use of Laboratory Animals. As another experiment, six FL-N/35 transgenic mice were fed the control diet for 6 months, and then they were divided into two groups: three fed the iron-excess diet for 6 months with administration of *N*-acetyl cysteine (NAC) and those without NAC. NAC was contained in drinking water (1 g/L).

Hepatic iron and triglyceride content

Iron concentrations in the livers were measured by atomic absorption spectrometry (Hitachi Z-6100, Hitachi Ltd., Tokyo, Japan), as described previously (9), and expressed as μg Fe/g of tissue (wet weight). Lipids were extracted from the homogenized liver tissue by the method of Bligh and Dyer (12). The triglyceride levels were measured with a TGE-test Wako kit (Wako Pure Chemicals, Tokyo, Japan) according to the manufacturer's instructions. The protein concentrations in the liver were determined by the method of Lowry *et al.* (13), using a DC protein assay kit (Bio-Rad Laboratories, Hercules, CA, USA).

Immunoblotting

Lysates of liver were separated by sodium dodecyl sulphate-polyacrylamide gel electrophoresis. The proteins were transferred to polyvinylidene difluoride membranes (Millipore, Bedford, MA, USA), blocked overnight at 4 °C with 5% skim milk and 0.1% Tween 20 in Tris-buffered saline and subsequently incubated for 1 h at room temperature with an anti-human ferritin antibody (Dako, Glostrup, Denmark), anti-rabbit carnitine palmitoyl transferase I (CPT I) antibody, anti-rabbit CPT II antibody (Alpha Diagnostic International, San Antonio, TX, USA), anti-rabbit SREBP1 antibody (Santa Cruz Biotechnology Inc., Santa Cruz, CA, USA), anti-rabbit fatty acid synthetase (FAS) antibody (Cell Signaling Technology Inc., Boston, MA, USA), anti-mouse X-box DNA-binding protein 1 (XBP-1) antibody (Santa Cruz Biotechnology Inc.) or anti-bacterially expressed, mouse CCAAT/enhancer-binding protein homology protein (CHOP) fusion protein antibody (Abcam, Cambridge, England). Exceptionally, the proteins were blocked for 1 h at room temperature and subsequently incubated overnight at 4 °C with an anti-rabbit phosphorylated eukaryotic initiation factor-2α (p-eIF2α) antibody (Cell Signaling Technology Inc.).

Histological staining

A portion of liver was immediately snap frozen in liquid nitrogen for determination of hepatic triglyceride and iron concentrations. The remaining liver tissue was fixed in 4% paraformaldehyde in phosphate-buffered saline and embedded in paraffin for histological analysis. Liver sections were stained with haematoxylin and eosin.

Electron microscopy

Liver specimens were fixed in 2.1% glutaraldehyde, post-fixed in 1% osmium tetroxide, dehydrated in graded ethanol and propylene dioxide and embedded in Epok. Thick sections (1 μm in width) were stained with toluidine blue to identify steatosis by light microscopy. Thin sections were stained with uranyl acetate and lead citrate, and examined using a Hitachi-7000 transmission electron microscope (Hitachi Ltd.).

In situ detection of reactive oxygen species

In situ ROS production in the liver was assessed by staining with dihydroethidium, as described previously (8). In the presence of ROS, dihydroethidium (Invitrogen Corp., Carlsbad, CA, USA) is oxidized to ethidium bromide and stains nuclei bright red by intercalating with the DNA (14). Fluorescence intensity was quantified using NIH image analysis software for three randomly selected areas of digital images in each mouse.

Statistical analysis

Quantitative values are expressed as mean ± SD. Two groups among multiple groups were compared by the rank-based, Kruskal–Wallis ANOVA test, followed by the Scheffé test. Data between two groups were compared by Student's *t*-test. The statistical significance of correlation was determined by the use of a simple regression analysis. A P value of < 0.05 was considered to be significant.

Results

Correlation between iron and triglyceride contents in the liver

Dietary intake and body weight were measured every 4 weeks until 12 months after commencement of iron loading, and these parameters did not differ significantly among any of the 4 groups. The hepatic iron content (267 ± 94 μg/g liver weight) of FL-N/35 transgenic mice fed the iron-excess diet was significantly greater than that of nontransgenic and FL-N/35 transgenic mice fed the control diet at 12 months after commencement of iron loading (Fig. 1A), and was comparable to that of a large number of patients with chronic hepatitis C in extensive studies (15, 16). The hepatic ferritin level of FL-N/35 transgenic mice fed the iron-excess diet was significantly greater than that of nontransgenic mice fed the control diet (Fig. 1B). The hepatic iron content was positively correlated with the hepatic triglyceride concentration when both parameters were compared for all mice ($r = 0.63$, $P = 0.002$, Fig. 1C). These results were consistent with our previous observation that FL-N/35 transgenic mice fed the iron-excess diet demonstrated the most severe steatosis in the liver among the four groups (9).

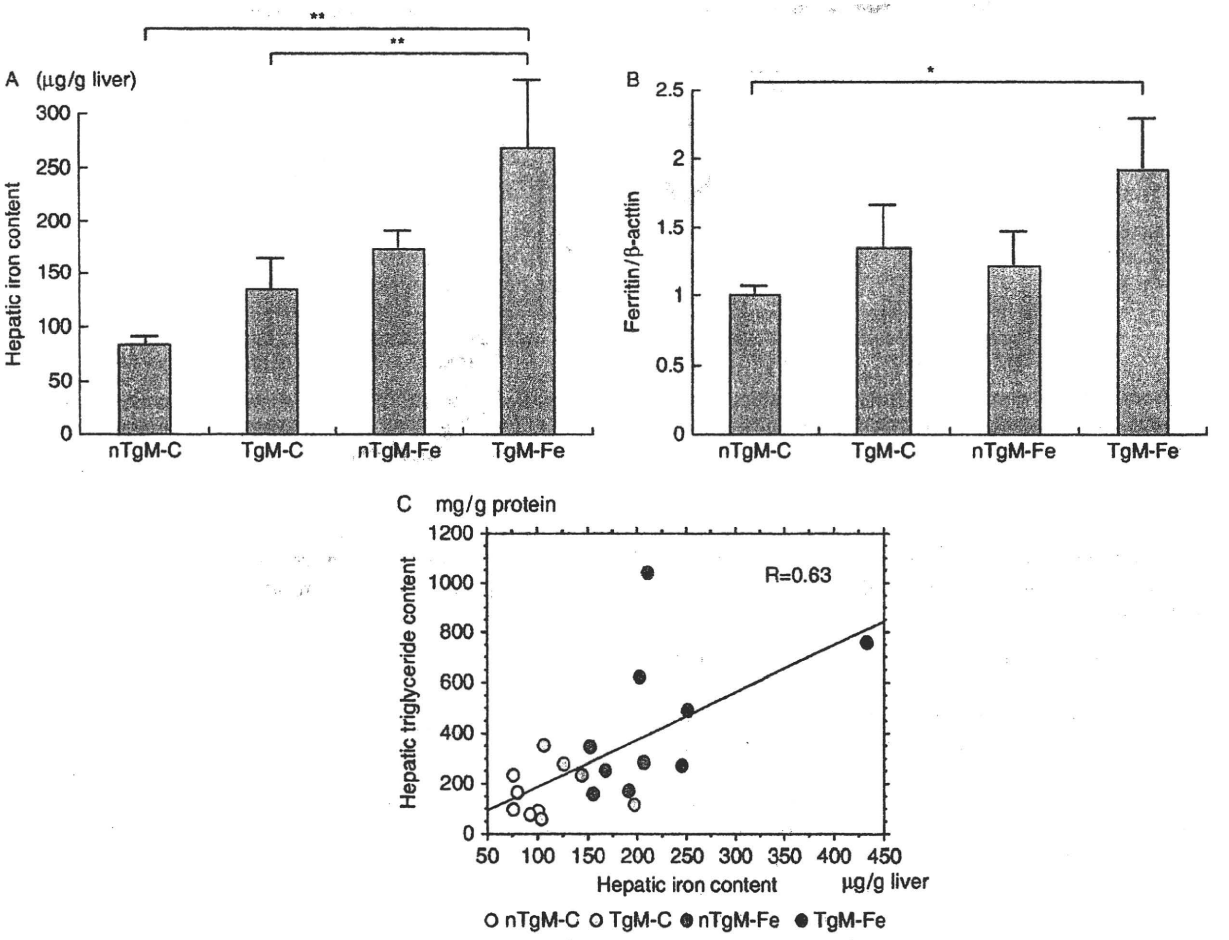

Fig. 1. Hepatic iron contents and ferritin levels, and correlation between iron and triglyceride contents in the liver. (A) The hepatic iron content was measured by atomic absorption spectrometry in five mice in each group at 12 months after initiation of iron loading. (B) Immunoblots for ferritin were performed using liver lysates obtained from four mice in each group. The protein expression was normalized with β-actin. (C) The correlation between hepatic iron and triglyceride levels was determined in 20 mice from four groups. nTgM-C: nontransgenic mice fed the control diet, nTgM-Fe: nontransgenic mice fed the iron-excess diet, TgM-C: FL-N/35 transgenic mice fed the control diet, TgM-Fe: FL-N/35 transgenic mice fed the iron-excess diet. $^{*}P < 0.05$, $^{**}P < 0.01$.

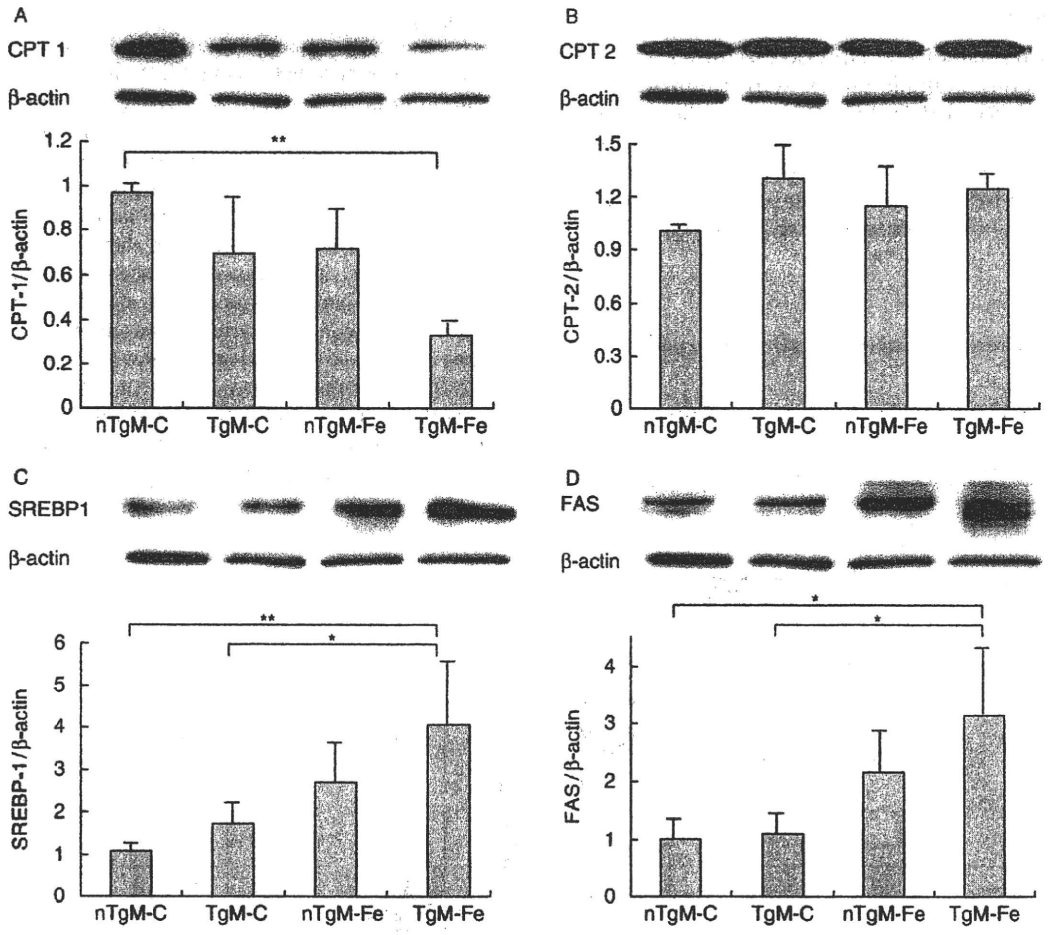

Fig. 2. Expression of carnitine palmitoyl transferase I (CPT1), carnitine palmitoyl transferase I (CPT2), sterol-regulatory element-binding protein I (SREBP1) and fatty acid synthetase (FAS) in the liver. Immunoblots for CPT1 (A), CPT2 (B), SREBP1 (C) and FAS (D) were performed using liver lysates obtained from four mice in each group at 12 months after initiation of iron loading. The protein expression was normalized with β-actin. $^{*}P < 0.05$, $^{**}P < 0.01$. nTgM-C, TgM-C, nTgM-Fe and TgM-Fe; see legend for Figure 1.

Decreased expression of carnitine palmitoyl transferase I and increased expression of sterol-regulatory element-binding protein 1

As we previously reported reduced oxidation activity of fatty acid in iron-overloaded transgenic mice (9), we first examined the expression levels of CPT1 and CPT2, which regulate oxidation of long-chain fatty acids in the mitochondria. The expression of CPT1, but not CPT2, was significantly reduced in FL-N/35 transgenic mice fed the iron-excess diet compared with the nontransgenic mice fed the control diet ($P = 0.0003$, Fig. 2A and B). We next examined the expression level of SREBP1, a transcription factor that activates the genes required for lipogenesis (17), and FAS, a target gene of SREBP1. As shown in Figures 2C and D, the expression of SREBP1 and FAS was significantly greater in FL-N/35 transgenic mice fed the iron-excess diet than in nontransgenic and FL-N/35 transgenic mice fed the control diet, suggesting the involvement of activated lipogenesis in hepatic steatosis in FL-N/35 transgenic mice fed the iron-excess diet. It should also be noted that modest iron supplementation significantly activated lipogenesis in FL-N/35 transgenic mice, but not in nontransgenic mice.

Activated unfolded protein response

Upon endoplasmic reticulum (ER) stress, the SREBP–SREBP cleavage-acting protein (SCAP) complex dissociates from the ER retention protein and subsequently translocates to the Golgi apparatus, where SREBP is cleaved and activated (18, 19). We therefore investigated whether increased expression of SREBP1 was related to ER stress. The unfolded protein response-signalling cascades are initiated by three ER-resident sensors: inositol-requiring enzyme 1 (IRE1), RNA-activated protein kinase (PKR)-like ER kinase (PERK) and activating transcription factor 6 (ATF6) (20). IRE1 activation splices unspliced XBP-1 (uXBP-1) to form spliced XBP-1 (sXBP-1) mRNA (21),

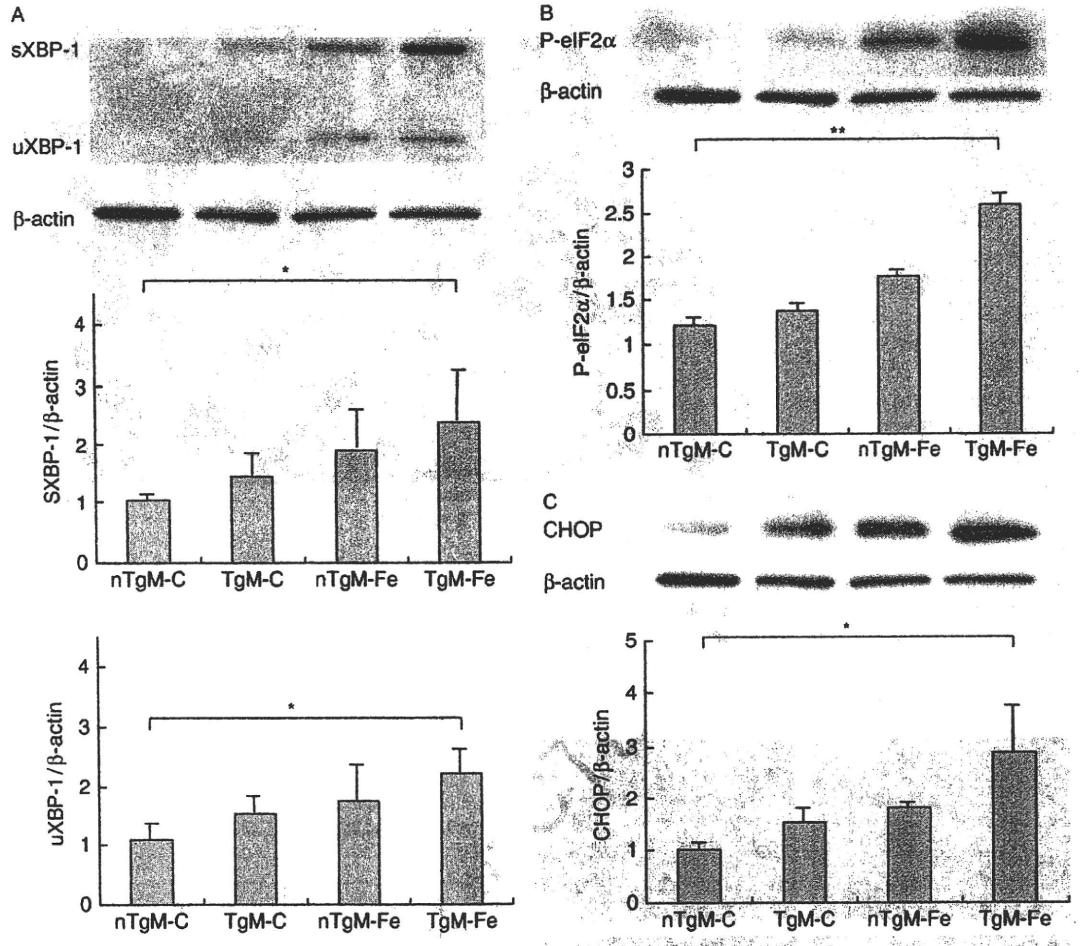

Fig. 3. Expression of spliced X-box DNA-binding protein 1 (sXBP-1), unspliced X-box DNA-binding protein 1 (uXBP-1), phosphorylated eukaryotic initiation factor-2α (p-eIF2α) and CCAAT/enhancer-binding protein homology protein (CHOP) in the liver. Immunoblots for sXBP-1 and uXBP-1 (A), p-eIF2α (B) and CHOP (C) were performed using liver lysates obtained from seven full-length HCV-N open reading frame (FL-N/35) transgenic mice fed the iron-excess diet and four mice in the three other groups at 12 months after initiation of iron loading. The protein expression was normalized with β-actin. $^{*}P < 0.05$, $^{**}P < 0.01$. nTgM-C, TgM-C, nTgM-Fe, and TgM-Fe; see legend for Figure 1.

and was assessed with the sXBP-1 protein level (22). PERK activation was evaluated by measurement of p-eIF2α and CHOP (23). ATF6 activation was assessed with uXBP-1 expression (24). The expression of uXBP-1, sXBP1, p-eIF2α and CHOP was significantly greater in FL-N/35 transgenic mice fed the iron-excess diet than that in nontransgenic mice fed the control diet (Fig. 3).

Autophagy

We next examined the formation of autophagosomes at the ultrastructural level to confirm the activation of the unfolded protein response, because autophagy has been shown to be induced by the unfolded protein response (25–27). As shown in Figure 4, autophagosomes (indicated by arrows) were abundantly found in the liver in FL-N/35 transgenic mice fed the iron-excess diet. In contrast, autophagosomes were not present in the liver of nontransgenic mice fed the iron-excess diet. These results were compatible with the increased expression of uXBP1, sXBP1, p-eIF-2α and CHOP in FL-N/35 transgenic mice fed the iron-excess diet, suggesting activation of the unfolded protein response. Thus, activation of the unfolded protein response appeared to be involved in the development of hepatic steatosis in FL-N/35 transgenic mice fed the iron-excess diet.

Reactive oxygen species generation and endoplasmic reticulum stress

Superoxide has been reported to be selectively involved in ER stress-mediated apoptosis (28). It is also reported that anti-oxidants reduce ER stress and improve protein secretion (29). These results suggest that ROS production induces ER stress. We evaluated *in situ* ROS production in the liver by staining with dihydroethidium and assessed whether treatment with an anti-oxidant reduced hepatic steatosis through inhibition of the unfolded protein response. ROS production was significantly higher in FL-N/35

LIV 2210

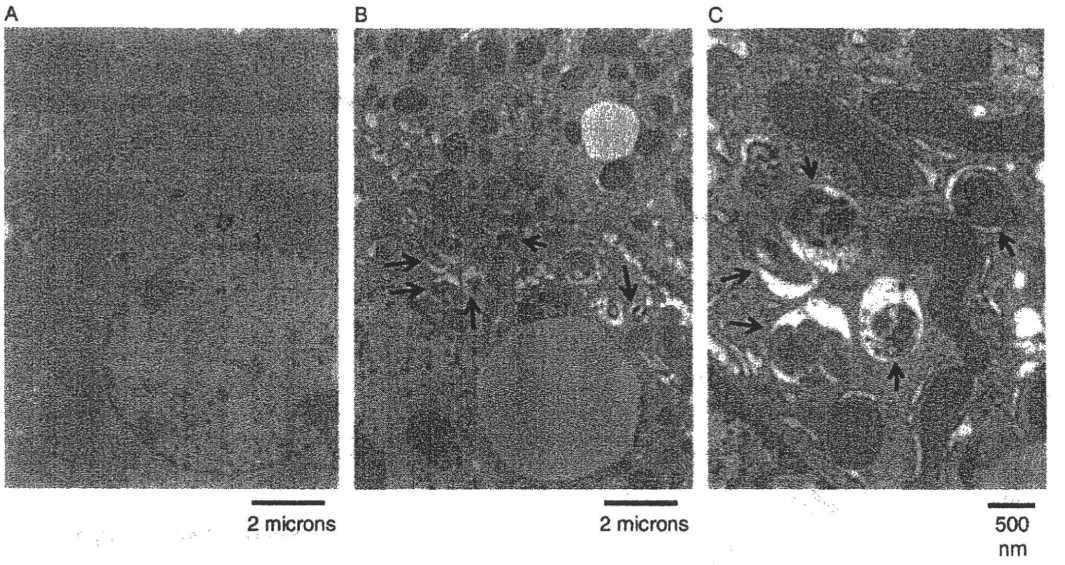

Fig. 4. Electron microscopy of the liver of an FL-N/35 transgenic mouse and a nontransgenic mouse, both of which were fed the iron-excess diet for 12 months. (A) Nontransgenic mouse, (B) full-length HCV-N open reading frame (FL-N/35) transgenic mouse and (C) Magnified picture of B. Autophagosomes (indicated by arrows) are abundantly found in the liver of the FL-N/35 transgenic mouse fed the iron-excess diet. Magnification scales are indicated below each picture.

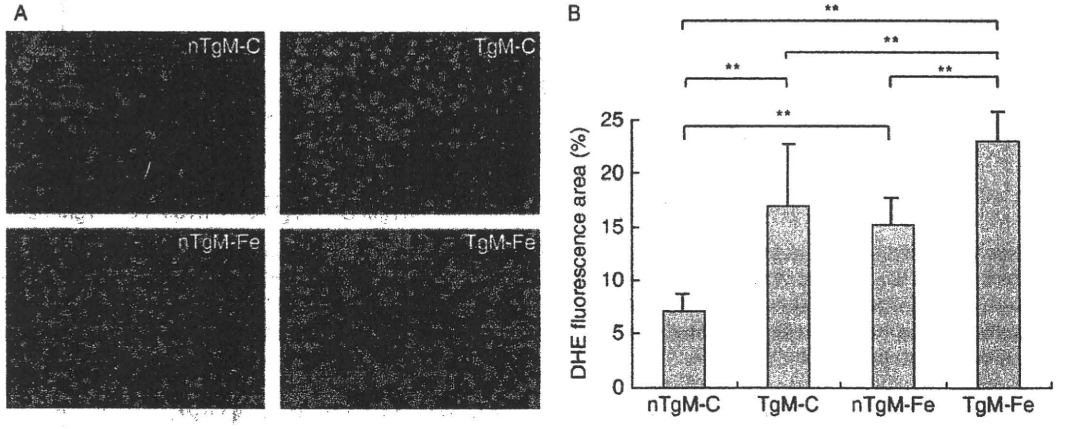

Fig. 5. Reactive oxygen species production in the liver. (A) Frozen liver sections of mice in each group were stained with dihydroethidium. (B) Fluorescence intensity was quantified by NIH image analysis software for three randomly selected areas of digital images for three mice in each group at 12 months after initiation of iron loading. $^{**}P < 0.01$. nTgM-C, TgM-C, nTgM-Fe, and TgM-Fe; see legend for Figure 1.

transgenic mice fed the iron-excess diet than in mice in the three other groups, even though abundant ROS production was found in all mice, except for nontransgenic mice fed the control diet (Fig. 5A and B). ROS production was significantly higher in transgenic mice than in nontransgenic mice irrespective of iron overloading. Iron overloading also significantly increased ROS production irrespective of whether the mice were transgenic or nontransgenic (Fig. 5B). FL-N/35 transgenic mice fed the iron-excess diet had the highest level of ROS production.

A six-month treatment with an anti-oxidant, NAC, dramatically reduced hepatic steatosis in FL-N/35 transgenic mice fed the iron-excess diet (Fig. 6A), together

Fig. 6. Liver histology, and the ratio of liver weight to body weight, serum alanine aminotransferase (ALT) levels, reactive oxygen specie's production and expression of carnitine palmitoyl transferase I (CPT1), sterol-regulatory element-binding protein I (SREBP1), spliced X-box DNA-binding protein 1 (sXBP1), unspliced X-box DNA-binding protein 1 (uXBP1) and CCAAT/enhancer-binding protein homology protein (CHOP) in the liver of full-length HCV-N open reading frame (FL-N/35) transgenic mouse fed the iron-excess diet with/without *N*-acetyl cysteine (NAC) treatment. (A) NAC treatment drastically reduced hepatic steatosis in mice. (B) Frozen liver sections of mice in each group were stained with dihydroethidium. Fluorescence intensity was quantified with the method described in the legend for Figure 5 in three mice in each group. (C)

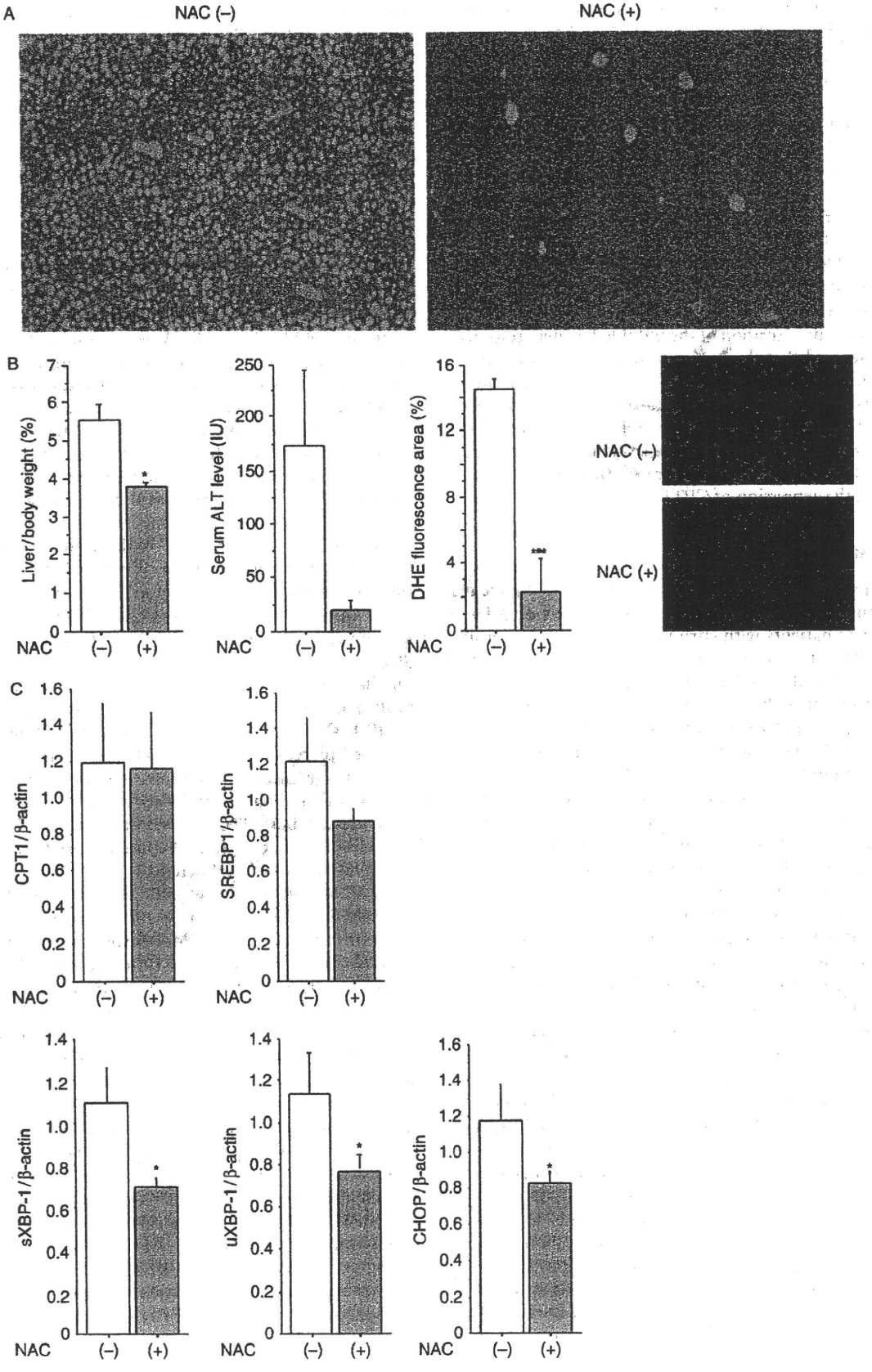

Colour

with a significant reduction in the ratio of liver weight to body weight and ROS production (Fig. 6B). The serum alanine aminotransferase level was also reduced by NAC, but this change was not statistically significant because of the large variance of the data. The expression of uXBP1, sXBP1 and CHOP was significantly reduced after treatment with NAC, suggesting an inhibitory effect of the anti-oxidant on the unfolded protein response (Fig. 6C). The expression of SREBP1 was also reduced by treatment with NAC, but this reduction was not statistically significant ($P = 0.08$). The expression of CPT1, which regulates oxidization of long-chain fatty acids in the mitochondria, did not change after NAC treatment. These results suggested that iron-induced ROS generation induced hepatic steatosis through the activation of the unfolded protein response. It also seemed that the increased lipogenesis through the activated unfolded protein response contributed more to the development of hepatic steatosis than the reduced β-oxidation activity in FL-N/35 transgenic mice fed the iron-excess diet, because the anti-oxidant almost completely inhibited the development of hepatic steatosis without affecting the expression of CPT1.

Discussion

The hepatic iron content of FL-N/35 transgenic mice fed the iron-excess diet was comparable to that of a large number of patients with chronic hepatitis C in extensive studies (15, 16). The positive correlation between the iron level and the triglyceride concentration in the liver was consistent with our previous observation that even modest iron supplementation enhanced hepatic steatosis in FL-N/35 transgenic mice (9), suggesting a potential role of iron in the development of HCV-related steatosis. Although previous studies revealed a direct contribution of HCV core protein to the development of hepatic steatosis (5–7), how iron overload, which is one of pathological features in chronic hepatitis C, affects hepatic steatosis remains unknown. The decreased expression of CPT I suggested reduced β-oxidation activity, because this transmembrane enzyme of the mitochondrial outer membrane has been shown to be the rate-limiting step in the β-oxidation of long-chain fatty acids (30). This result was consistent with our previous observation that the degradation activity of fatty acids *in vivo* was reduced in iron-overloaded transgenic mice. The decreased expression of CPT I may be related to the association of HCV core protein with the mitochondrial outer membrane (31). However, the decreased expression of CPT I seemed to reflect the rather increased synthesis of fatty acids because CPT I is negatively regulated by malonyl-CoA, an intermediate product in fatty acid synthesis, at the transcriptional level (30). In fact, the expression of FAS was significantly increased in FL-N/35 transgenic mice fed the iron-excess diet, which was presumably driven by upregulation of a transcription factor, SREBP1. We could not differentiate SREBP1c from SREBP1a at the protein level because of the lack of an adequate antibody; nevertheless, the expression of SREBP1 was assumed to mainly reflect that of SREBP1c, because the SREBP1c transcript extremely predominates over the SREBP1a transcript is considerably predominant in the mouse liver (32).

The regulation of SREBP activation occurs at two levels: transcriptional and post-transcriptional (17). Upregulation of SREBP1c promoter activity has been reported in HCV core gene-transgenic mice (6), but we did not find a significant difference in SREBP1 expression between transgenic and nontransgenic mice without iron overloading. This contradiction may have arisen from a difference in the transgenic mice used in the two studies. In addition, a recent report found no significant difference in the hepatic expression of SREBP1c mRNA between subjects with HCV infection and those with a histologically normal liver (33). HCV has been demonstrated to induce proteolytic cleavage of SREBP1 and 2 in HCV replicon cells (34). As described previously, modest iron supplementation restored a major phenotype of FL-N/35 transgenic mice marked by hepatic steatosis and liver tumour development (9). Thus, the present animal model was useful for understanding the critical role of iron overloading in the development of HCV-related hepatic steatosis. We therefore focused on the post-transcriptional regulation of SREBP1 by iron in the presence of HCV proteins. Upon ER stress, the SREBP–SCAP complex dissociates from the ER retention protein and subsequently translocates to the Golgi apparatus, where SREBP is cleaved and activated (18, 19). FL-N/35 transgenic mice fed the iron-excess diet showed the activated unfolded protein response, assessed by the increased expression of uXBP-1, sXBP-1, p-eIF2α and CHOP, suggesting that the unfolded protein response was activated by iron overloading in the presence of HCV proteins. On the other hand, it is demonstrated that the trans-activating activity of XBP-1 is suppressed, but ATF6 functions properly in HCV replicon cells (35), which is in part contradictory to the present results. Methodological differences (*in vivo* or *in vitro*, iron overload or not, etc.) in two studies may account for this contradiction. Thus, the role of the unfolded protein response in HCV infection alone is still a matter of debate.

To confirm activation of the unfolded protein response in FL-N/35 transgenic mice fed the iron-excess diet, we wanted to assess not only the activation of ER-resident sensors but also the morphological change induced by the unfolded protein response. Autophagy has been shown to play important roles in cell survival after ER stress (25–27). A double-membrane structure, which is called the autophagosome or the autophagic vacuole, is formed *de novo* to sequester cytoplasm. Then the vacuole membrane fuses with the lysosomal membrane to deliver the contents into the autolysosome, where they are degraded and the resulting macromolecules are recycled. Some studies demonstrated a critical role of IRE1 in inducing autophagy under ER stress (25, 36), whereas another study reported the involvement of the PERK-eIF2α signalling pathway, not IRE1, in autophagy induction by ER stress (37). Thus, it is still controversial as to

which transducer is utilized for ER stress-induced autophagy in mammalian cells. The abundant presence of autophagosomes was consistent with the activation of both ER-resident sensors, IRE1 and PERK, in the liver in FL-N/35 transgenic mice fed the iron-excess diet. Although there is no direct link between induction of autophagy and hepatic steatosis in FL-N/35 transgenic mice fed the iron-excess diet, induction of autophagy seemed to support the ER stress-related hepatic steatosis because autophagy is one of the morphological changes under ER stress (25–27).

Iron overload is potentially one of multiple sources of ROS production, as represented in the iron-catalysed Fenton reaction (38). FL-N/35 transgenic mice fed the iron-excess diet had a significantly higher level of ROS production than mice in the three other groups, suggesting a cooperative role of HCV proteins and iron in inducing oxidative stress. ROS have been demonstrated to be involved upstream of the unfolded protein response (28). Anti-oxidants have also been shown to reduce the unfolded protein response and improve protein secretion (29). The present findings that the expression of uXBP1, sXBP1 and CHOP, but not CPT1, was significantly reduced with NAC treatment were consistent with these previous observations, suggesting that iron-induced ROS activated the unfolded protein response in the presence of HCV proteins. How then does ER stress activate SREBP1? There are several lines of evidence suggesting that one mechanism by which ER stress leads to activation of SREBPs is related to downregulation of insulin-induced genes. Downregulation of insulin-induced genes is associated with less retention of SREBPs in the ER, which leads to increased SREBP activation (39–41). As another mechanism, it has been shown that overexpression of glucose-regulated protein 78, one of the ER resident chaperone proteins, inhibits SREBP activation (42). Irrespective of how ER stress activates SREBP, the predominant role of SREBP1 in the ER stress-related hepatic steatosis in FL-N/35 transgenic mice fed the iron-excess diet was similar to that observed in a murine intragastric ethanol-feeding model (43). In conclusion, considering the complexity of the argument and the limited number of evaluated mechanisms, iron-induced ROS-activated unfolded protein response may be postulated as one of the possible mechanisms of HCV-related fat accumulation in the liver.

Acknowledgements

This study was supported by a grant from the Ministry of Education, Culture, Sports, Science and Technology (No. 20590782), and in part by the Ministry of Health, Labor and Welfare, Japan.

References

1. Scheuer PJ, Ashrafzadeh P, Sherlock S, Brown D, Dusheiko GM. The pathology of hepatitis C. *Hepatology* 1992; **15**: 567–71.
2. Farinati F, Cardin R, De Maria N, *et al.* Iron storage, lipid peroxidation and glutathione turnover in chronic anti-HCV positive hepatitis. *J Hepatol* 1995; **22**: 449–56.
3. Ohata K, Hamasaki K, Toriyama K, *et al.* Hepatic steatosis is a risk factor for hepatocellular carcinoma in patients with chronic hepatitis C virus infection. *Cancer* 2003; **97**: 3036–43.
4. Kato J, Kobune M, Nakamura T, *et al.* Normalization of elevated hepatic 8-hydroxy-2′-deoxyguanosine levels in chronic hepatitis C patients by phlebotomy and low iron diet. *Cancer Res* 2001; **61**: 8697–702.
5. Perlemuter G, Sabile A, Letteron P, *et al.* Hepatitis C virus core protein inhibits microsomal triglyceride transfer protein activity and very low density lipoprotein secretion: a model of viral-related steatosis. *FASEB J* 2002; **16**: 185–94.
6. Moriishi K, Mochizuki R, Moriya K, *et al.* Critical role of PA28γ in hepatitis C virus-associated steatogenesis and hepatocarcinogenesis. *Proc Natl Acad Sci USA* 2007; **104**: 1661–6.
7. Tanaka N, Moriya K, Kiyosawa K, *et al.* PPARα activation is essential for HCV core protein-induced hepatic steatosis and hepatocellular carcinoma in mice. *J Clin Invest* 2008; **118**: 683–94.
8. Nishina S, Hino K, Korenaga M, *et al.* Hepatitis C virus-induced reactive oxygen species raise hepatic iron level in mice by reducing hepcidin transcription. *Gastroenterology* 2008; **134**: 226–38.
9. Furutani T, Hino K, Okuda M, *et al.* Hepatic iron overload induces hepatocellular carcinoma in transgenic mice expressing the hepatitis C virus polyprotein. *Gastroenterology* 2006; **130**: 2087–98.
10. Beard MR, Abell G, Honda M, *et al.* An infectious molecular clone of a Japanese genotype 1b hepatitis C virus. *Hepatology* 1999; **30**: 316–24.
11. Lerat H, Honda M, Beard MR, *et al.* Steatosis and liver cancer in transgenic mice expressing the structural and nonstructural proteins of hepatitis C virus. *Gastroenterology* 2002; **122**: 352–65.
12. Bligh EG, Dyer WJ. A rapid method of total lipid extraction and purification. *Can J Biochem Physiol* 1959; **37**: 911–7.
13. Lowry OH, Rosebrough NJ, Farr AL, Randall RJ. Protein measurement with the Folin phenol reagent. *J Biol Chem* 1951; **193**: 265–75.
14. Harrison-Findik DD, Schafer D, Klein E, *et al.* Alcohol metabolism-mediated oxidative stress down-regulates hepcidin transcription and leads to increased duodenal iron transporter expression. *J Biol Chem* 2006; **281**: 22974–82.
15. Hofer H, Osterreicher C, Jessner W, *et al.* Hepatic iron concentration does not predict response to standard and pegylated-IFN/ribavirin therapy in patients with chronic hepatitis C. *J Hepatol* 2004; **40**: 1018–22.
16. Rulyak SJ, Eng SC, Patel K, *et al.* Relationships between hepatic iron content and virologic response in chronic hepatitis C patients treated with interferon and ribavirin. *Am J Gastroenterol* 2005; **100**: 332–7.
17. Horton JD, Goldstein JL, Brown MS. SREBPs: activators of the complete program of cholesterol and fatty acid synthesis in the liver. *J Clin Invest* 2002; **109**: 1125–31.

18. Brown MS, Goldstein JL. The SREBP pathway: regulation of cholesterol metabolism by proteolysis of a membrane-bound transcription factor. *Cell* 1997; **89**: 331–40.
19. Ron D, Oyadomari S. Lipid phase perturbations and the unfolded protein response. *Dev Cell* 2004; **7**: 287–8.
20. Ji C, Kaplowitz N. ER stress: can the liver cope? *J Hepatol* 2006; **45**: 321–33.
21. Calfon M, Zeng H, Urano F, *et al.* IRE1 couples endoplasmic reticulum load to secretory capacity by processing the XBP-1 mRNA. *Nature* 2002; **415**: 92–6.
22. Yoshida H, Matsui T, Yamamoto A, Okada T, Mori K. XBP1 mRNA is induced by ATF6 and spliced by IRE1 in response to ER stress to produce a highly active transcription factor. *Cell* 2001; **107**: 881–91.
23. Marciniak SJ, Ron D. Endoplasmic reticulum stress signaling in disease. *Physiol Rev* 2006; **86**: 1133–49.
24. Okada T, Yoshida H, Akazawa R, Negishi M, Mori K. Distinct roles of activating transcription factor 6 (ATF6) and double-stranded RNA-activated protein kinase-like endoplasmic reticulum kinase (PERK) in transcription during the mammalian unfolded protein response. *Biochem J* 2002; **366**: 585–94.
25. Ogata M, Hino S, Saito A, *et al.* Autophagy is activated for cell survival after endoplasmic reticulum stress. *Mol Cell Biol* 2006; **26**: 9220–31.
26. Yorimitsu T, Nair U, Yang Z, Klionsky DJ. Endoplasmic reticulum stress triggers autophagy. *J Biol Chem* 2006; **281**: 30299–304.
27. Yin XM, Ding WX, Gao W. Autophagy in the liver. *Hepatology* 2008; **47**: 1773–85.
28. Yokouchi M, Hiramatsu N, Hayakawa K, *et al.* Involvement of selective reactive oxygen species upstream of proapoptotic branches of unfolded protein response. *J Biol Chem* 2008; **283**: 4252–60.
29. Malhotra JD, Miao H, Zhang K, *et al.* Antioxidants reduce endoplasmic reticulum stress and improve protein secretion. *Proc Natl Acad Sci USA* 2008; **105**: 18525–30.
30. Kerner J, Hoppel C. Fatty acid import into mitochondria. *Biochim Biophys Acta* 2000; **1486**: 1–17.
31. Korenaga M, Wang T, Li Y, *et al.* Hepatitis C virus core protein inhibits mitochondrial electron transport and increases reactive oxygen species (ROS) production. *J Biol Chem* 2005; **280**: 37481–8.
32. Shimomura I, Shimano H, Horton JD, Goldstein JL, Brown MS. Differential expression of exons 1a and 1c in mRNAs for sterol regulatory element binding protein-1 in human and mouse organs and cultured cells. *J Clin Invest* 1997; **99**: 838–45.
33. McPherson S, Jonsson JR, Barrie HD, *et al.* Investigation of the role of SREBP-1c in the pathogenesis of HCV-related steatosis. *J Hepatol* 2008; **49**: 1046–54.
34. Waris G, Felmlee DJ, Negro F, Siddiqui A. Hepatitis C virus induces proteolytic cleavage of sterol regulatory element binding proteins and stimulates their phosphorylation via oxidative stress. *J Virol* 2007; **81**: 8122–30.
35. Tardif KD, Mori K, Kaufman RJ, Siddiqui A. Hepatitis C virus suppresses the IRE1-XBP1 pathway of the unfolded protein response. *J Biol Chem* 2004; **279**: 17158–64.
36. Yorimitsu T, Klionsky DJ. Endoplasmic reticulum stress: a new pathway to induce autophagy. *Autophagy* 2007; **3**: 160–2.
37. Kouroku Y, Fujita E, Tanida I, *et al.* ER stress (PERK/eIF2alpha phosphorylation) mediates the polyglutamine-induced LC3 conversion, an essential step for autophagy formation. *Cell Death Differ* 2007; **14**: 230–9.
38. Fenton HJH. Oxidation of tartaric acid in presence of iron. *J Chem Soc* 1894; **65**: 899–910.
39. Engelking LJ, Kuriyama H, Hammer RE, *et al.* Overexpression of Insig-1 in the livers of transgenic mice inhibits SREBP processing and reduces insulin-stimulated lipogenesis. *J Clin Invest* 2004; **113**: 1168–75.
40. Engelking LJ, Liang G, Hammer RE, *et al.* Schoenheimer effect explained – feedback regulation of cholesterol synthesis in mice mediated by Insig proteins. *J Clin Invest* 2005; **115**: 2489–98.
41. Flury I, Garza R, Shearer A, *et al.* INSIG: a broadly conserved transmembrane chaperone for sterol-sensing domain proteins. *EMBO J* 2005; **24**: 3917–26.
42. Werstuck GH, Lentz SR, Dayal S, *et al.* Homocysteine-induced endoplasmic reticulum stress causes dysregulation of the cholesterol and triglyceride biosynthetic pathways. *J Clin Invest* 2001; **107**: 1263–73.
43. Ji C, Chan C, Kaplowitz N. Predominant role of sterol response element binding proteins (SREBP) lipogenic pathways in hepatic steatosis in the murine intragastric ethanol feeding model. *J Hepatol* 2006; **45**: 717–24.

J Gastroenterol 2007; 42:168–175
DOI 10.1007/s00535-006-1963-2

Journal of Gastroenterology

Case report

A male patient with severe acute hepatitis who was domestically infected with a genotype H hepatitis B virus in Iwate, Japan

Ichiro Kumagai[1], Koichi Abe[1], Takayoshi Oikawa[1], Akihiro Sato[1], Shinichiro Sato[1], Ryujin Endo[1], Yasuhiro Takikawa[1], Kazuyuki Suzuki[1], Tomoyuki Masuda[2], Shigehiko Sainokami[1,3], Kazunori Endo[4], Masaharu Takahashi[4], and Hiroaki Okamoto[4]

[1]First Department of Internal Medicine, Iwate Medical University, Iwate, Japan
[2]Second Department of Pathology, Iwate Medical University, Iwate, Japan
[3]Division of Liver Diseases, Oshu City Hospital, Iwate, Japan
[4]Division of Virology, Department of Infection and Immunity, Jichi Medical University School of Medicine, 3311-1 Yakushiji, Shimotsuke, Tochigi 329-0498, Japan

Although all eight genotypes of hepatitis B virus (HBV) strains are circulating in Japan, no cases of acute hepatitis with foreign HBV strains of genotype H have thus far been reported in Japan. Here, we report a 35-year-old Japanese patient with severe acute hepatitis who was domestically infected with genotype H HBV. On admission, he had a high HBV load of 1.0×10^9 copies/ml, elevated levels of total bilirubin (7.0 mg/dl) and alanine aminotransferase (3606 IU/l), and reduced prothrombin activity of 39.0%. The HB-JAIW05 isolate obtained in the present study was composed of 3215 nucleotides and had the highest similarity of 99.7% with the reported genotype H HBV isolate recovered from a Japanese blood donor. The HB-JAIW05 isolate had neither precore (A1896) nor core promoter (T1762/A1764) mutations. However, upon comparison with the consensus sequence of ten reported HBV isolates of the same genotype, the HB-JAIW05 isolate had 17 nucleotide substitutions including five missense mutations in the *P* gene, which may be related to vigorous replication of HBV in this case. He had no history of traveling abroad, but had had extramarital sexual contact with two Japanese women living in Iwate, Japan, 2 weeks and 2 months before the disease onset, respectively. Our results suggest that rare HBV genotypes such as H may be spreading in Japan via sexual contact. Further molecular epidemiological studies on HBV to clarify the exact changing profiles of de novo HBV infection in Japan in relation to genotype and genomic variability are warranted.

Key words: severe acute hepatitis, hepatitis B virus, genotype H

Received: August 9, 2006 / Accepted: September 21, 2006
Reprint requests to: H. Okamoto

Introduction

Hepatitis B virus (HBV) is one of the most important causes of acute and chronic liver diseases worldwide, including acute self-limited hepatitis, fulminant hepatitis, chronic hepatitis, liver cirrhosis, and hepatocellular carcinoma. HBV possesses a circular, partially double-stranded DNA genome of approximately 3200 nucleotides (nt). It contains four major open reading frames encoding the envelope [preS1, preS2 and surface antigen (HBsAg)], precore/core antigen (HBeAg and HBcAg), polymerase (P), and X (HBx) proteins. Eight genotypes of HBV, A to H, have thus far been recognized,[1–4] and have different geographical distributions.[5–8] Genotype A is found predominantly in northwestern Europe, North America, and central Africa. Genotypes B and C are found in Southeast Asia, China, and Japan, whereas genotype D has a worldwide distribution but is predominant in the Mediterranean area, the Middle East, and India. Genotype E occurs frequently in Africa, whereas genotype F is found among American natives and in Polynesia and Central and South America. Genotype G HBV has been reported in France, Germany, the United States, and Mexico. The eighth genotype, named H, a newly described genotype, was considered to be confined to Latin America,[4] but it has been found not only in Nicaragua and Mexico but also in the United States and Japan.[4,9–13] Five of the genotypes, A, B, C, D, and F, have been further subdivided into subgenotypes, which are identified by Arabic numbers.[6,7]

In Japan, genotypes B and C are predominant, and genotypes A, D, and F are found in small percentages of HBV-viremic blood donors and patients with chronic HBV infection;[14,15] genotypes E, G, and H have rarely been found in patients infected with human immunodeficiency virus type 1 (HIV).[11] Since the successful

implementation of a nationwide program preventing mother-to-infant infection of HBV by administering hepatitis B immune globulins and HB vaccines to newborns[16] and nationwide nucleic acid amplification testing (NAT) of voluntarily donated blood for HBV, hepatitis C virus (HCV), and HIV by the Japanese Red Cross Blood Transfusion Services,[17,18] a major cause of acute HBV infection in Japan is sexual contact with HBV-viremic partners. A recent study indicated that genotype A HBV prevails among Japanese patients with acute hepatitis B, particularly in metropolitan areas of Japan.[19] However, no patients with acute hepatitis who were infected with foreign HBV strains of genotype H have thus far been reported in Japan. Here, we report a patient with severe acute hepatitis who was domestically infected with a genotype H HBV, most likely via sexual contact with Japanese women living in Iwate, a nonmetropolitan area located in the northern part of Honshu Island, Japan.

Case report

Methods

All routine hematological and biochemical examinations were performed using an autoanalyzer. The presence of hepatitis B surface antigen (HBsAg) and the corresponding antibody (anti-HBs), hepatitis B e antigen (HBeAg) and antibody to HBeAg (anti-HBe), antibody to hepatitis B core (anti-HBc), IgM class anti-HBc and IgM class antibody to hepatitis A virus (IgM anti-HAV) was tested by chemiluminescence enzyme immunoassay using kits from Fuji Rebio (Tokyo, Japan). Third-generation antibody to HCV (anti-HCV) was measured by chemiluminescence immunoassay (Ortho Diagnostic Systems, Tokyo, Japan). IgG and IgM classes of antibodies to Epstein-Barr virus, cytomegalovirus, human parvovirus B19, human herpesvirus type 6, and varicella zoster virus were assayed by the fluorescent antibody method using the respective commercial kits.

The presence of HBV DNA was determined by polymerase chain reaction (PCR) with nested primers targeting the *S* gene of the HBV genome according to the method described previously.[20] The amplification product of the first-round PCR was 461 base pairs (bp), and that of the second-round PCR was 437 bp. Quantitation of HBV DNA was performed by real-time detection PCR using the LightCycler-FastStart DNA Master Hybridization Probes kit (Roche Diagnostics, Mannheim, Germany) as described previously.[21]

The presence of antibodies to hepatitis D virus (HDV) was determined by in-house enzyme-linked immunosorbent assay (ELISA), using purified recombinant S-HDAg protein that had been expressed in the pupae of silkworm, as described previously.[22] IgG, IgM, and IgA classes of antibodies to hepatitis E virus (HEV) (IgG anti-HEV, IgM anti-HEV and IgA anti-HEV, respectively) were assayed by in-house ELISA as described previously.[23]

The entire nucleotide sequence of the HBV genome was determined by methods essentially similar to those described previously.[24] Briefly, three overlapping regions of HBV DNA were amplified by nested PCR with TaKaRa *Ex Taq* (TaKaRa Bio, Shiga, Japan) and the appropriate primers derived from conserved areas of the genomes of the eight genotypes (A to H). The three overlapping regions (primer sequences at both ends excluded) that were amplified spanned nt 265–1795 (1531 bp), nt 1674–2380 (707 bp), and nt 2282–3215 and 1–458 (1392 bp). The amplification products were sequenced directly on both strands using the BigDye Terminator Cycle Sequencing Ready Reaction Kit on an ABI PRISM 3100 Genetic Analyzer (Applied Biosystems, Foster City, CA, USA). Sequence analysis was performed using Genetyx-Mac version 12.2.5 (Genetyx, Tokyo, Japan) and ODEN version 1.1.1 from the DNA Data Bank of Japan (DDBJ: National Institute of Genetics, Mishima, Japan).[25] Phylogenetic trees were constructed by the neighbor-joining method.[26] Bootstrap values were determined on 1000 resamplings of the data sets.[27]

Profile and clinical course of the present case

The patient was a 35-year-old Japanese man. He noticed dark urine, general fatigue, and anorexia in August 2005. On the following day, he consulted a physician in private practice, and abnormalities on liver function tests were found. Two days later, he was hospitalized at a local hospital. However, his symptoms worsened, and his prothrombin activity was markedly low. He was transferred to the Iwate Medical University Hospital 2 days later. He had no history of blood transfusion, travel abroad, excessive intake of alcohol, or drug abuse. However, he had had extramarital sexual contact with two Japanese women living in Iwate Prefecture, Japan, 2 weeks and 2 months, respectively, before the onset of the disease.

On admission, he had severe jaundice in the bulbar conjunctiva and skin, but he was alert and there were no abnormal vital signs. Physical examination revealed no lymphadenopathy, hepatomegaly, splenomegaly, ascites, or edema. Laboratory findings on admission showed markedly elevated serum total bilirubin and liver enzyme levels, and low serum albumin and total cholesterol levels. Prothrombin activity was remarkably low, and the human hepatocyte growth factor level was moderately elevated (Table 1). Screening tests for hepatitis virus markers revealed positivity for HBsAg and

Table 1. Laboratory findings on admission

Parameter	Value	Parameter	Value
Hematology		Viral markers	
White blood cells	8230/μl	IgM anti-HAV (C.O.I.)	0.2 (–)
Red blood cells	487×10^4/μl	IgM anti-HBc (C.O.I.)	31.2 (+)
Hemoglobin	15.7 g/dl	HBsAg (C.O.I.)	>2000 (+)
Platelets	14.8×10^4/μl	Anti-HBs (C.O.I.)	0.5 (–)
Blood chemistry		HBeAg (C.O.I.)	319.2 (+)
Total protein	6.5 g/dl	Anti-HBe	71.6% (+)
Albumin	3.6 g/dl	Anti-HBc	100% (+)
Total bilirubin	7.0 mg/dl	Anti-HBc (1:200 dilution)	97.5% (+)
Direct bilirubin	5.4 mg/dl	HBV DNA (copies/ml)	1.0×10^9 (+)
AST	1679 IU/l	Anti-HCV (C.O.I.)	0.2 (–)
ALT	3606 IU/l	IgG anti-HDV (OD value)	0.014 (–)
LDH	643 IU/l	IgG anti-HEV (OD value)	0.014 (–)
ALP	527 IU/l	IgM anti-HEV (OD value)	0.203 (–)
γ-GTP	212 IU/l	IgA anti-HEV (OD value)	0.049 (–)
Total cholesterol	65 mg/dl	HEV RNA	(–)
IgG	1451 mg/dl	IgM antibody to EBV VCA	<1:10 (–)
IgA	176 mg/dl	IgG antibody to EBV VCA	1:80 (+)
IgM	330 mg/dl	Antibody to EBV EBNA	<1:10 (–)
NH_3	38 μg/dl	IgM antibody to CMV	<1:10 (–)
BUN	4.9 mg/dl	IgG antibody to CMV	1:10 (–)
Creatinine	0.6 mg/dl	IgM antibody to B19	(–)
Na	37 mEq/l	IgG antibody to B19	(+)
K	4.0 mEq/l	IgM antibody to HSV	<1:10 (–)
Cl	106 mEq/l	IgG antibody to HSV	1:80 (+)
Coagulation tests and others		IgM antibody to HHV-6	<1:10 (–)
Prothrombin time	18.8 s (39.0%)	IgG antibody to HHV-6	1:40 (+)
Fibrinogen	210.6 mg/dl	IgM antibody to VZV	(–)
hHGF	0.75 ng/ml	IgG antibody to VZV	(+)

AST, aspartate aminotransferase; ALT, alanine aminotransferase; LDH, lactic dehydrogenase; ALP, alkaline phosphatase; γ-GTP, γ-glutamyl transpeptidase; BUN, Blood urea nitrogen; hHGF, human hepatocyte growth factor; C.O.I., cutoff index; HAV, hepatitis A virus; anti-HBc, antibody to hepatitis B core; HBsAg, hepatitis B surface antigen; anti-HBs, antibody to HBsAg; HBeAg, hepatitis B e antigen; anti-HBe, antibody to HBeAg; HBV, hepatitis B virus; HCV, hepatitis C virus; HDV, hepatitis D virus; HEV, hepatitis E virus; EBV VCA, Epstein-Barr virus viral capsid antigen; EBNA, Epstein-Barr nuclear antigen; CMV, cytomegalovirus; B19, human parvovirus B19; HSV, herpes simplex virus; HHV-6, human herpesvirus type 6; VZV, varicella zoster virus; OD, optical density

IgM anti-HBc, but negativity for anti-HBs antibody. HBeAg and anti-HBe antibody were both positive. The HBV DNA titer in the circulation was markedly high at 1.0×10^9 copies/ml. IgM antibodies against hepatitis A, C, D, and E viruses and other viruses, including Epstein-Barr virus, cytomegalovirus, human parvovirus B19, herpes simplex virus, human herpes virus type 6, and varicella zoster virus, which are known to be related to hepatic injury, were all negative (Table 1). Furthermore, anti-nuclear antibody and anti-mitochondria antibody were negative. Abdominal computed tomography and ultrasonography showed no signs of hepatic failure such as liver atrophy, irregular density of the liver, or ascites, but did reveal slight splenomegaly and the collapse and thickening of the wall of the gallbladder, which are found in patients with acute hepatitis. Based on these results, he was diagnosed as having severe acute hepatitis B due to de novo HBV infection.

Figure 1 illustrates the clinical course of the patient after admission. Although he did not receive artificial liver support or any antiviral drug, his consciousness level and general condition did not deteriorate and his transaminase levels and prothrombin activity gradually improved. Laparoscopy performed on day 22 of admission showed no macroscopic abnormalities of the liver. Histological examination of the biopsied liver specimens showed slight infiltration of mononuclear cells in the portal area unaccompanied by fibrosis. He was discharged on day 33. During the course of his illness, the serum HBV DNA level gradually decreased and became undetectable (<30 copies/ml) on day 159. HBsAg became negative on day 86.

Analysis of the full-length genomic sequence of HBV

The full-length genomic sequence of an HBV isolate (HB-JAIW05) obtained from the present case was determined and deposited in the DDBJ/GenBank/EMBL databases (accession no. AB266536). The HB-JAIW05 isolate had a total genomic length of 3215 nt, which is

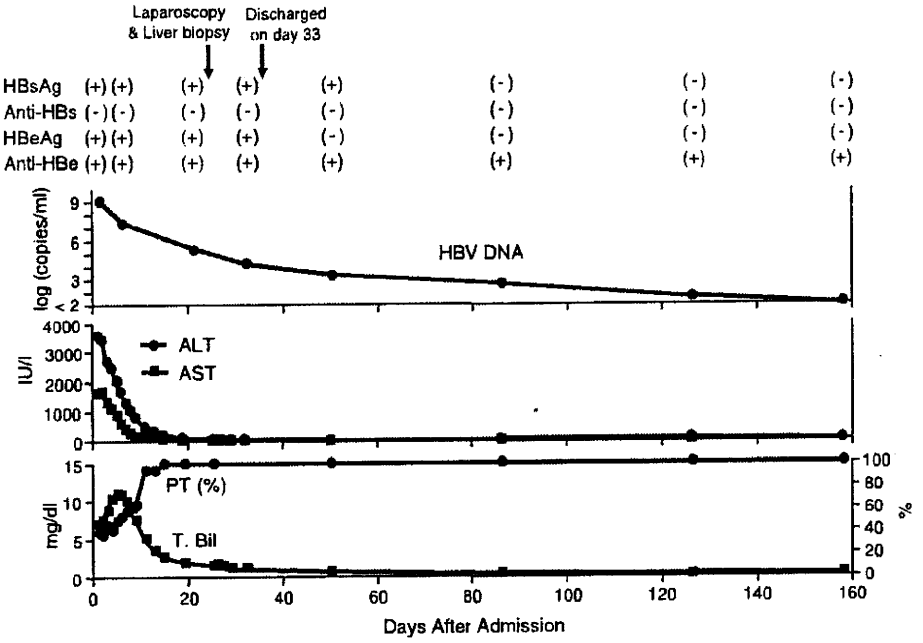

Fig. 1. Laboratory parameters and hepatitis B virus markers in serum samples that were periodically obtained from the patient with severe acute hepatitis B. The patient was admitted to our hospital on day 0 and discharged on day 33. *ALT*, alanine aminotransferase; *AST*, aspartate aminotransferase; *PT*, prothrombin activity; *T. Bil*, total bilirubin; HBsAg, hepatitis B surface antigen; Anti-HBs, antibody to hepatitis B surface antigen; HBeAg, hepatitis B e antigen; Anti-HBe, antibody to hepatitis B e antigen

identical to that of reported HBV isolates of genotypes B, C, F, and H. When the entire nucleotide sequence was compared with the reported genomes of all eight genotypes for which the full-length sequence is known, the HB-JAIW05 isolate was most closely related to the genotype H isolates with identities of 97.4%–99.7%, was close to the genotype F isolates with identities of 91.0%–92.8%, but was only 84.5%–86.8% identical to the HBV isolates of the remaining six genotypes (A, B, C, D, E, and G). Among the ten genotype H strains isolated in the United States, Nicaragua, and Japan whose full-length sequence has been determined, the HB-JAIW05 isolate had the highest similarity of 99.7% with the HB-JBDH1 isolate recovered from a Japanese blood donor whose viremia was identified by nucleic acid amplification testing and who presumably donated blood during the serological window period at an early stage of de novo infection.[12]

A phylogenetic tree was constructed based on the entire genomic sequence of 53 HBV isolates (including the HB-JAIW05 isolate obtained in the present study), which confirmed that the HB-JAIW05 isolate segregated into genotype H (Fig. 2). Close relatedness of HB-JAIW05 with the reported HBV strains of genotype H and clear branching of the eight genotypes were observed.

The HB-JAIW05 isolate had neither precore (preC, nt 1896) nor core promoter (nt 1762, 1764) mutations (A1896, T1762/A1764 mutation, respectively). Upon comparison with the consensus sequence of ten reported HBV isolates of the same genotype (for accession nos., see Fig. 2), the HB-JAIW05 isolate had 17 nucleotide substitutions that resulted in five amino acid substitutions in the *P* gene product, two amino acid substitutions in the *X* gene product, and one each in the preS2 region and *S* gene products (Table 2).

Discussion

In the present study, we reported a 35-year-old Japanese man with severe acute hepatitis who was infected with a genotype H HBV and had never been abroad. In Japan, a recent nationwide survey revealed the frequencies of various HBV genotypes among 301 patients with acute hepatitis B: genotype C was most prevalent (67%), followed by genotype B (15%), genotype A (14%), genotype G (2%), and genotype D (2%).[28] In addition to this large-scale survey, many reports on the distribution of HBV genotypes among patients with acute hepatitis in Japan have recently been published;[19,29–33] however, there have been no patients with acute hepatitis who were infected with a genotype H HBV, suggesting that this is the first report of an acute hepatitis patient in Japan who contracted infection of a genotype H HBV domestically.

Eight genotypes of HBV are currently recognized.[1–4] Each HBV genotype shows a distinct geographical distribution between and even within regions, and such data are an invaluable tool in tracing the molecular evolution and patterns and modes of spread of HBV.[5–8] Among the eight genotypes, genotype H has most recently been identified from two Nicaraguans and one American living in Los Angeles,[4] and has also been

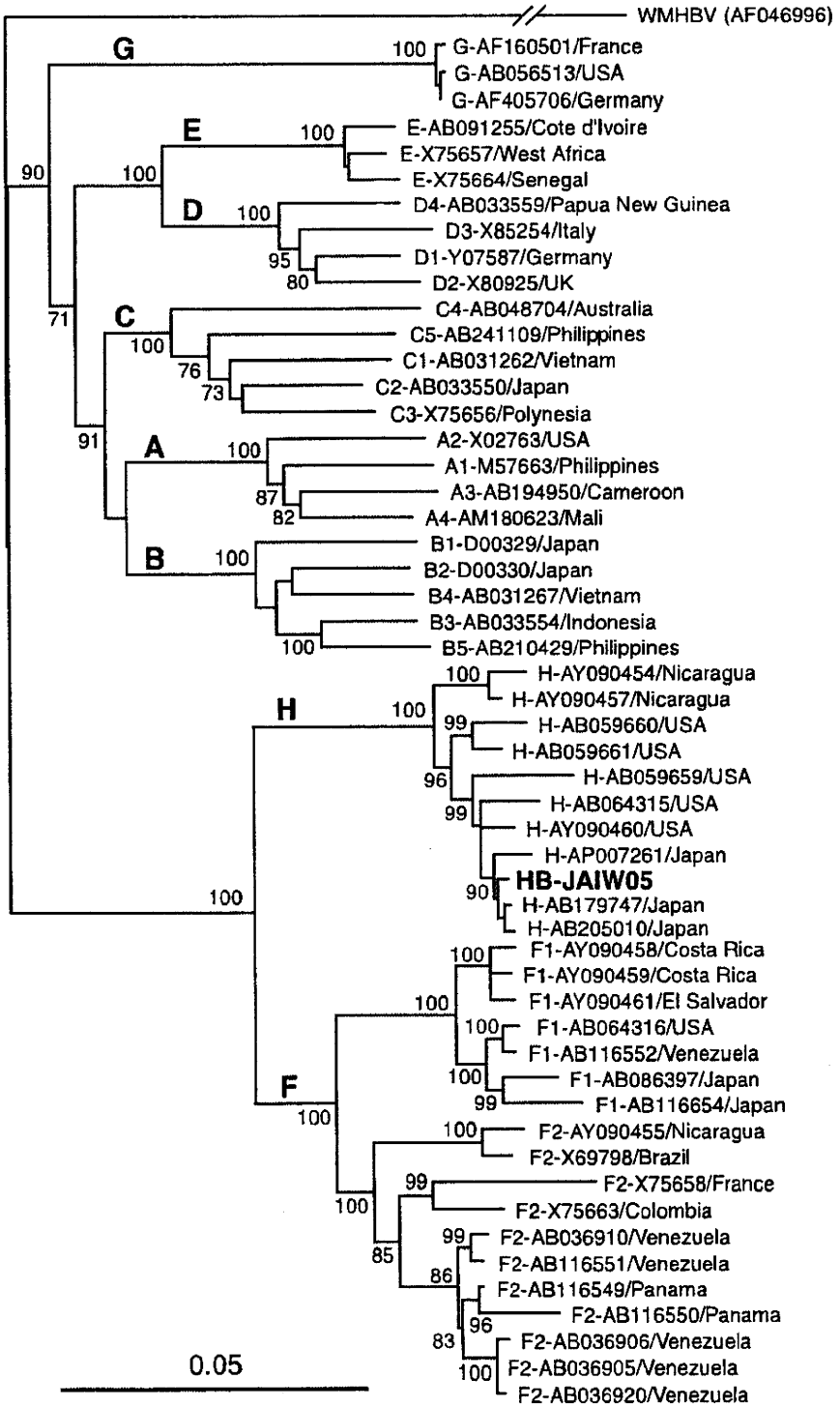

Fig. 2. Phylogenetic tree constructed by the neighbor-joining method based on the entire nucleotide sequence of 53 hepatitis B virus (HBV) isolates, using a woolly monkey HBV isolate (WMHBV: AF046996) as an out-group. In addition to the HB-JAIW05 isolate obtained from the patient with severe acute hepatitis B in the present study, indicated in bold type for visual clarity, 24 representative HBV isolates of genotypes *A* to *E* and *G* and all 18 genotype *F* and 10 genotype *H* isolates whose entire sequence is known were included for comparison. The previously reported isolates are indicated with the genotype or subgenotype and accession no., followed by the name of the country where it was isolated. Bootstrap values are indicated for the major nodes as a percentage of the data obtained from 1000 resamplings

encountered in Mexico and San Francisco.[9,10] However, the nature of HBV genotype H throughout the world remains obscure. In Japan, genotype H is very rarely found, and only three genotype H isolates have thus far been reported. Shibayama et al.[11] reported that a genotype H strain (HB-JI260; accession no. AP007261) was isolated from a 46-year-old Japanese patient coinfected with HIV who had a history of traveling to South America and had had a sexual relationship there.[11] Nakajima et al.[13] isolated a genotype H strain (HBV-IM806-2; AB205010) from a 61-year-old Japanese patient with chronic hepatitis, who while visiting Bangkok, Thailand, 30 years earlier had had a sexual relationship with a woman there, and 3 months after returning to Japan acquired acute hepatitis, which developed into chronic hepatitis B. In addition, the

Table 2. Sequence comparison between the HBV clone from this case and the consensus sequence from ten reported HBV clones of the same genotype (genotype H)

Nt position	Nt change	Genomic region	Amino acid change
46	T to G	preS2, P	—, Ser319 to Ala319 (P)
147	C to T	preS2, P	Ala53 to Val53 (preS2), —
242	C to A	S, P	Gln30 to Lys30 (S), Thr384 to Lys384 (P)
747	T to C	S, P	—, —
851	T to C	P	—
868	T to C	P	—
870	A to T	P	—
1164	G to A	P	—
1287	A to C	P	—
1306	C to A	P	—
1386	C to T	P, X	—, —
1504	C to T	P, X	Pro805 to Ser805 (P), Ala44 to Val44 (X)
1632	C to T	X	Arg87 to Trp87 (X)
2035	C to A	C	—
2101	C to A	C	—
2410	A to T	C, P	—, His35 to Leu35 (P)
2505	G to A	P	Val67 to Ile67 (P)

Nt, nucleotide

Japanese Red Cross NAT Screening Research Group reported that HBV genotype H has been found in only one (0.3%) of 328 HBV DNA-positive blood donors in Japan, and that the genotype H isolate (HB-JBDH1; AB179747) was recovered from a 52-year-old Japanese man who donated blood in October 2002.[12] These results and our present result indicate that individuals infected with a genotype H HBV are rare, but may serve as possible infectious sources in Japan.

The number of cases of acute HBV infection in Japan is estimated to be over 10000 cases per year. More than 50% of patients with acute hepatitis B had extramarital sexual contact within a period of time corresponding to the incubation period before the development of acute hepatitis B,[34] indicating that a major cause of acute HBV infection in Japan is sexual intercourse with an HBV-viremic partner. The precise reason why genotype A HBV has become prevalent among Japanese patients with acute hepatitis B remains unknown. However, the decreasing rates of mother-to-baby transmission and transfusion-associated transmission of genotypes B and C along with the increasing risk of sexual transmission may be involved in the changing pattern of the distribution of HBV genotypes in Japan, and rare HBV genotypes that are not found in chronic HBV carriers would become prevalent among individuals with high sexual activity with diverse partners, some of whom may be infected with various blood-borne viruses, including HIV and HBV, and even among individuals with sexual relationships with commercial sex workers, who are at high risk for contracting infection of blood-borne viruses. The present patient had extramarital sexual contact with two Japanese women living in Iwate, who were not commercial sex workers, 2 weeks and 2 months before the disease onset, respectively, although it remains unknown whether they were infected with HBV. The present case occurring in a nonmetropolitan area suggests that rare HBV genotypes such as genotype H may be widely distributed in Japan. Extensive molecular epidemiological surveys on the distribution of HBV genotype are needed to clarify the exact changing profile of de novo HBV infection in Japan and to develop programs to prevent acute HBV infection.

Severe acute hepatitis is defined as acute hepatitis having reduced prothrombin activity of <40% but without overt hepatic encephalopathy (coma grade > II). Our case had a prothrombin activity level of 39% on admission, but, fortunately, he did not develop hepatic encephalopathy. A nationwide survey that evaluated the outcome of severe acute hepatitis indicated that 31% of 164 patients with severe acute hepatitis developed overt encephalopathy and were diagnosed as having fulminant hepatic failure.[34] Therefore, prothrombin activity is one of the most important markers for predicting the development of hepatic encephalopathy in patients with acute hepatitis. Besides prolonged prothrombin time, old age and an elevated total bilirubin level were estimated to be potential risk factors for developing encephalopathy among patients with severe acute hepatitis.[34] However, our patient was young (35 years old) and his total bilirubin level was only moderately elevated (7.0 mg/dl). These findings may be consistent with his good clinical course. Recent studies have shown that the genotype of HBV is closely associated with the pathogenesis and clinical outcome of HBV-related liver diseases.[35–37] Viral factors may also play a

role in the pathogenesis of severe acute hepatitis or fulminant hepatitis. HBV variants with mutations in the precore region (A1896) and/or the core promoter (T1762 and A1764) have been implicated in fulminant hepatitis.[38-42] It is possible that the frequency of genomic mutations differs according to genotype. However, the particular genomic mutations in genotype H HBV that are associated with the severe or fulminant form of acute hepatitis or exacerbation of chronic liver disease are not known. Although the HB-JAIW05 isolate was recovered from a patient with severe acute hepatitis B in the present study, neither precore mutation (A1896) nor double mutations in the core promoter region (T1762/A1764) were present. When compared with the consensus sequence of all ten reported genotype H HBV strains whose entire sequence is known, including two Nicaraguan isolates, five Californian isolates, and three Japanese isolates, 17 nucleotide substitutions unique to the HB-JAIW05 isolate were recognized. The 17 nucleotide changes included five missense mutations (amino acids 35, 67, 319, 384, and 805) in the *P* gene, which may be associated with vigorous replication of HBV as observed at the time of admission of the present patient (1.0×10^9 copies/ml). Although further studies on a greater number of patients with acute hepatitis who are infected with genotype H HBV are required, these 17 nucleotide substitutions in HBV DNA could be candidates for mutations associated with the severe or fulminant form of acute hepatitis.

In conclusion, we identified and determined the full-length sequence of a genotype H HBV (HB-JAIW05) that had been recovered from a 35-year-old Japanese patient with severe acute hepatitis, who was presumed to have contracted the disease via sexual contact with Japanese women living in Iwate, a nonmetropolitan area in the northern part of Honshu Island. Our results suggest that rare HBV genotypes such as H may be spreading in Japan via sexual contact. Further molecular epidemiological studies on HBV infection are warranted to clarify the changing profiles of de novo HBV infection in Japan in relation to genotype and genomic variability.

References

1. Okamoto H, Tsuda F, Sakugawa H, Sastrosoewignjo RI, Imai M, Miyakawa Y, et al. Typing hepatitis B virus by homology in nucleotide sequence: comparison of surface antigen subtypes. J Gen Virol 1988;69:2575–83.
2. Norder H, Courouce AM, Magnius LO. Complete genomes, phylogenetic relatedness, and structural proteins of six strains of the hepatitis B virus, four of which represent two new genotypes. Virology 1994;198:489–503.
3. Stuyver L, De Gendt S, Van Geyt C, Zoulim F, Fried M, Schinazi RF, et al. A new genotype of hepatitis B virus: complete genome and phylogenetic relatedness. J Gen Virol 2000;81:67–74.
4. Arauz-Ruiz P, Norder H, Robertson BH, Magnius LO. Genotype H: a new Amerindian genotype of hepatitis B virus revealed in Central America. J Gen Virol 2002;83:2059–73.
5. Miyakawa Y, Mizokami M. Classifying hepatitis B virus genotypes. Intervirology 2003;46:329–38.
6. Norder H, Courouce AM, Coursaget P, Echevarria JM, Lee SD, Mushahwar IK, et al. Genetic diversity of hepatitis B virus strains derived worldwide: genotypes, subgenotypes, and HBsAg subtypes. Intervirology 2004;47:289–309.
7. Kramvis A, Kew M, Francois G. Hepatitis B virus genotypes. Vaccine 2005;23:2407–21.
8. Chu CJ, Keeffe EB, Han SH, Perrillo RP, Min AD, Soldevila-Pico C, et al. Hepatitis B virus genotype in the United States: results of a nationwide study. Gastroenterology 2003;125:444–51.
9. Kato H, Gish RG, Bzowej N, Newsom M, Sugauchi F, Tanaka Y, et al. Eight genotypes (A–H) of hepatitis B virus infecting patients from San Francisco and their demographic, clinical, and virological characteristics. J Med Virol 2004;73:516–21.
10. Sanchez LV, Maldonado M, Bastidas-Ramírez BE, Norder H, Panduro A. Genotypes and S-gene variability of Mexican hepatitis B virus strains. J Med Virol 2002;68:24–32.
11. Shibayama T, Masuda G, Ajisawa A, Hiruma K, Tsuda F, Nishizawa T, et al. Characterization of seven genotypes (A to E, G and H) of hepatitis B virus recovered from Japanese patients infected with human immunodeficiency virus type 1. J Med Virol 2005;76:24–32.
12. Ohnuma H, Yoshikawa A, Mizoguchi H, Okamoto H and JRC NAT Screening Research Group. Characterization of genotype H hepatitis B virus strain identified for the first time from a Japanese blood donor by nucleic acid amplification test. J Gen Viral 2005;86:595–9.
13. Nakajima A, Usui M, Huy TT, Hlaing NK, Masaki N, Sata T, et al. Full-length sequence of hepatitis B virus belonging to genotype H identified in a Japanese patient with chronic hepatitis. Jpn J Infect Dis 2005;58:244–6.
14. Usuda S, Okamoto H, Iwanari H, Baba K, Tsuda F, Miyakawa Y, et al. Serological detection of hepatitis B virus genotypes by ELISA with monoclonal antibodies to type-specific epitopes in the preS2-region product. J Virol Methods 1999;80:97–112.
15. Orito E, Ichida T, Sakugawa H, Sata M, Horiike N, Hino K, et al. Geographic distribution of hepatitis B virus (HBV) genotype in patients with chronic HBV infection in Japan. Hepatology 2001;34:590–4.
16. Shiraki K. Perinatal transmission of hepatitis B virus and its prevention. J Gastroenterol Hepatol 2000;15 Suppl:E11–5.
17. Ohnuma H, Tanaka T, Yoshikawa A, Murokawa H, Minegishi K, Yamanaka R, et al. The first large-scale nucleic acid amplification testing (NAT) of donated blood using multiplex reagent for simultaneous detection of HBV, HCV, and HIV-1 and significance of NAT for HBV. Microbiol Immunol 2001;45:667–72.
18. Mine H, Emura H, Miyamoto M, Tomono T, Minegishi K, Murokawa H, et al. High throughput screening of 16 million serologically negative blood donors for hepatitis B virus, hepatitis C virus and human immunodeficiency virus type-1 by nucleic acid amplification testing with specific and sensitive multiplex reagent in Japan. J Virol Methods 2003;112:145–51.
19. Yotsuyanagi H, Okuse C, Yasuda K, Orito E, Nishiguchi S, Toyoda J, et al. Distinct geographic distributions of hepatitis B virus genotypes in patients with acute infection in Japan. J Med Virol 2005;77:39–46.
20. Takahashi M, Nishizawa T, Gotanda Y, Tsuda F, Komatsu F, Kawabata T, et al. High prevalence of antibodies to hepatitis A and E viruses and viremia of hepatitis B, C, and D viruses among apparently healthy populations in Mongolia. Clin Diagn Lab Immunol 2004;11:392–8.
21. Akahane Y, Okada S, Sakamoto M, Wakamiya M, Kitamura T, Tawara A, et al. Persistence of hepatitis B viremia after recovery from acute hepatitis B: correlation between anti-HBc titer and HBV DNA in serum. Hepatol Res 2002;24:8–17.

has been reported that FH patients with detectable HBV DNA had a lower mortality rate than those without, and it has been considered that an enhanced immune response decreases the viral replication level,[1,3,14] suggesting that antiviral agents may not be useful for treating FH. In previous studies, HBV DNA assays were performed only after the onset of hepatic encephalopathy, not before it. Moreover, it has not been clarified yet how viral load and its changing pattern in the early phase are associated with the clinical outcome and whether the presence of precore or core promoter mutations correlates with viral load in patients with acute HBV infection.

In this study, we retrospectively quantified serum HBV DNA in 42 patients with acute HBV infection, the severity of which ranged from acute self-limited hepatitis to FH observed from the early phase of the clinical course, to assess whether viral load was an important factor for their prognosis, in relation to precore or core promoter mutations.

Patients and methods

Patients with acute HBV infection

Forty-two consecutive patients with acute HBV infection, who were admitted to Iwate Medical University Hospital from June 1990 to March 2005, were enrolled in this study. Patients who had been treated with antiviral drugs and those who had received blood transfusion (including plasma exchange) in a previous hospital after the disease onset were excluded from this study. Twenty-two patients were men, and the mean age ± standard deviation (SD) was 36 ± 17 years (range, 18–75 years). Aminotransferase activity peaked within 4 days after admission. Twenty-two patients had AH with a prothrombin activity equal to or greater than 40% of the control value during the clinical course; 9 patients had the severe form of acute hepatitis (SAH) with a reduced prothrombin activity of less than 40% of the control value, without hepatic encephalopathy during the clinical course; and 11 patients had FH with reduced prothrombin activity that was less than 40% of the control value. Signs of encephalopathy were present on admission in 9 patients and appeared within a week following admission in 2. Of these 11 patients, 7 patients became comatose within 7 days after the clinical onset of hepatitis. The appearance of early symptoms, such as fever, anorexia, malaise, nausea, vomiting, jaundice, and right hypochondrial discomfort, was defined as the clinical onset. Seven patients in deep coma and who did not undergo liver transplantation died of hepatic failure. The other 35 patients recovered spontaneously with a marked decrease in ALT activity and normal prothrombin activity.

Acute HBV infection was determined by either the appearance of hepatitis B surface antigen (HBsAg) or the detection of the high-titer immunoglobulin M (IgM) antibody to hepatitis B core antigen (anti-HBc IgM). All 42 patients were negative for antibody against hepatitis D virus. Although one female patient with FH was positive for antibody to hepatitis C virus (HCV), she had no HCV RNA detectable by reverse transcription-polymerase chain reaction (RT-PCR) assay. The study protocol conformed to the ethical guidelines of the 1975 Declaration of Helsinki and was approved by the Ethics Committee of Iwate Medical University, and informed consent was obtained from each patient or a family member of the patient. Serum samples, periodically collected from 31 patients after we had obtained their informed consent, were stored at –70°C until assay.

Serological markers of HBV infection and quantitation of HBV DNA

The presence of HBsAg was determined by radioimmunoassay (Authria-II-125; Abbott Japan, Tokyo, Japan) or enzyme-linked immunosorbent assay (ELISA; AxSYM; Abbott Japan). The presence of HBeAg and the corresponding antibody (anti-HBe) was determined by ELISA (AxSYM; Abbott Japan) or by chemiluminescence, using commercial assay kits (ARCHITECT; Abbott Japan). IgM class anti-HBc was detected by radioimmunoassay (Authria-II-125) or by chemiluminescence, using commercial assay kits (ARCHITECT). Serum HBV DNA was quantified by real-time detection PCR assay based on Taq Man chemistry (Operon Biotechnologies, Tokyo, Japan), as described previously.[15] All HBV DNA determinations were analyzed after $\log_{10}$ transformation. The linear range of this assay was 2.3–9.0 log (copies/ml). Samples with values exceeding 9.0 log (copies/ml) were considered to be above the linear range of the assay and were retested after a tenfold dilution, using normal human serum.

Genotypes and subgenotypes of HBV

The seven major HBV genotypes (A to G) were determined by a genotype-specific probe assay, using commercial kits (SMITEST HBV Genotype Detection kit; Genome Science Laboratories, Fukushima, Japan). This assay depends on the PCR products of the preS1 region of the HBV genome (nt 2902–3091) detected by hybridization with genotype-specific probes immobilized on a microwell plate.[16] For untypeable samples, the HBV genotype was determined by phylogenetic analysis of the S gene sequence, as described previously.[17]

The subgenotypes of Bj (Japanese type) without recombination with genotype C over the precore region and the core gene and Ba (Asian type) with the recombination were determined by the restriction fragment-